# A New Current Probe for Measuring Transient Events Under Data Traffic

Omid Hoseini Izadi (1), David Pommerenke (2), DongHyun Kim (1)

(1) EMC Laboratory, Missouri University of Science and Technology, 4000 Enterprise Dr., Rolla, MO, 65401, USA
tel.: 573-341-4730, fax: 573-341-4477, e-mail: ohp63@mst.edu

(2) Institute of Electronic, Graz University of Technology, Graz, Austria
e-mail: david.pommerenke@tugraz.at

***Abstract*** – Using inductive current measurement technique, a new current probe is proposed that allows transient current measurement on data traces without disturbing the normal operation or transfer rate of the trace under test. The proposed probe layout, circuit model, and frequency response is discussed in detail.

## I. Introduction

Measuring a transient event such as electrostatic discharge (ESD) on high-speed data traces such as USB or PCI Express (peripheral component interconnect express), during data traffic is not trivial. The use of any additional series component for this measurement may disturb the differential signaling by introducing enough parasitics to interfere with the normal functionality of the system, and hence disturb or even completely interrupt the data transfer.

One approach to measuring a transient current while minimally affecting the data traffic is to use a current probe such as a Tektronix CT1 or CT6 [1]. However, one cannot simply employ such probes on a differential data pairs on a printed circuit board (PCB) because the target trace cannot be separated from its return plane or its pair in order to provide enough clearance for these probes without disturbing the data transfer.

Another approach is to place a magnetic field probe on the trace, such as the one shown in figure 1, and obtain coupled voltage due to the transient event. Because of the derivative nature of these probes, the probe response has to be deconvolved from the measurements in order to reconstruct the actual current, as described in [2, 3].

Although this approach has a negligible impact on the data traffic due to the small coupling coefficient between the probe and the trace, the coupled voltage level strongly depends on the probe location, orientation, and distance from the trace under test. In a scenario where the trace width is comparable or smaller than the probe tip such as the one shown in figure 1, obtaining repeatable measurements can be difficult, as the magnetic field distribution around the trace varies significantly. A sub-millimeter change in the probe location and/or orientation can change the measured voltage level by several dBs. Therefore, any deviation from the exact location, orientation, and distance that the probe was originally characterized in, cause the measured voltage level to differ from the actual value. The impact of these dependencies can further increase as the trace gets narrower due to greater spatial field variation [4].

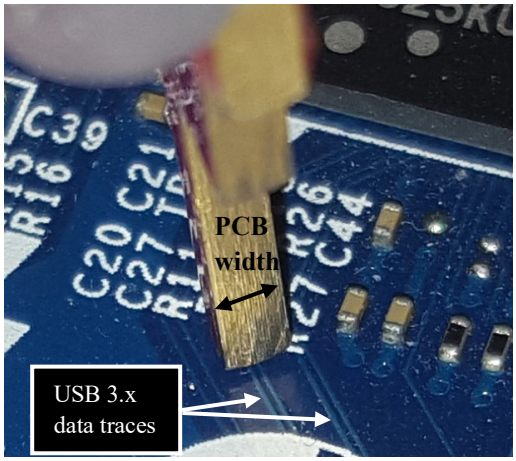


Figure 1: Comparing PCB width of a magnetic probe with a Gbps differential data pair. The probe has four layers. The probe loop could be either on layer 2, 3, or both; either way, the picked-up energy would largely depend on the location, orientation, and distance of the probe to the trance. Even if thinner PCB is used to reduce the effect of orientation, still the other two parameters affect the probe readouts.

In this paper, a new probe is proposed and fabricated for measuring transient currents in a data

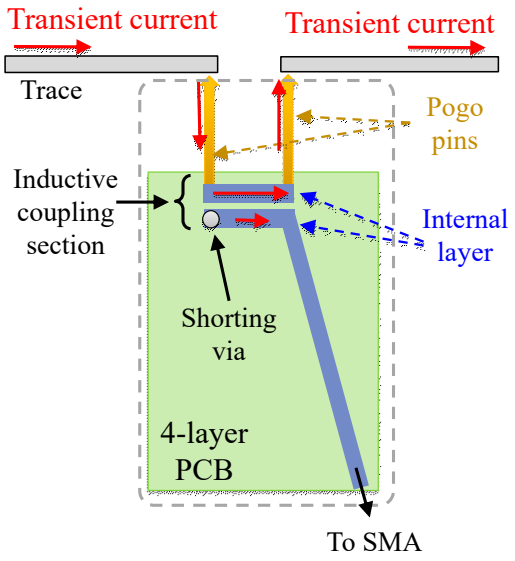


Figure 2: Illustration of a trace carrying transient current, and conceptual demonstration of the proposed probe with fixed coupling coefficient. The probe can be placed on the footprint of a zero-ohm resistor or on the trace, after making a small cut in the trace. (Drawing is not to scale.)

trace under data traffic. The traffic is minimally affected due to small mutual inductance between the probe and the trace under test (less than 300 pH). The designed probe introduces ~20 ps skew to the trace under test. This probe is named *Zero-Ohm substitution probe* by the authors, as it can substitute a zero-ohm resistor and measure the transient current. A simple circuit model is developed for this probe to estimate the probe response. This model is then used to deconvolve the probe's response from the measured current and reconstruct the actual time-domain transient current.

# II. Zero-Ohm Substitution Probe

## A. Coupling Section Design

The coupling coefficient between the probe and PCB trace is a strong function of probe location and orientation. By fixing the coupling coefficient (the proposed probe), we could remove the effect of positioning and obtain a stable reading. Figure 2 shows the conceptual illustration of the probe with a fixed inductive coupling section while measuring the transient current passing through the trace. The probe illustration is enclosed with the dashed line. Since the distance between the coupled traces is fixed, the probe reading does not depend on the probe location, orientation, or distance, as opposed to the probe in figure 1. This is the advantage of this probe over other magnetic probes, such as the one shown in figure 1.

The parasitic capacitance and inductance of the coupled section limit the upper usable frequency of the probe. Since most of the energy of an ESD event is below 1~2 GHz [3], the length of the coupled traces are designed to be 2.6 mm, through full-wave simulation to achieve a resonance-free response up to 2 GHz. The substrate used for this probe is FR4 with a relative permittivity of 3.5. Increasing the length of the coupled section allows more energy to get coupled to the probe; however, increasing the length beyond 4 mm results in a resonance below 2 GHz.

With a 2.6 mm coupling length and two 0.4-mm pogo pins, the total skew added to the trace due to the probe can be estimated by equation (1).

$$skew = \frac{2.6\,mm + 0.8\,mm}{\frac{1}{\sqrt{\varepsilon_r}}.c} \approx 21\,ps, \qquad (1)$$

where $c$ is the speed of light in free space, and $\varepsilon_r$ is the relative permittivity of the board. If the skew is not acceptable for an application, the length of the coupling section can be adjusted. However, a shorter length will result in a weaker coupling.

## B. Integrator Design

Since the coupling mechanism is derivative, an integrator is required to reconstruct the current waveform. This integrator should have a -20 dB/decades slope from a few kHz to 2 GHz, which means the integrator has to maintain its slope over ~6 decades; in other words, more than 120 dB dynamic range is required, which is not trivial to achieve.

Due to realization difficulties, the transient current is reconstructed in two steps: First, by using a one-pole low pass L-R filter over 1 or 2 decades, and second by deconvolving the probe response from the measured current waveform in the frequency domain to obtain the actual current waveform. The latter is explained in the current reconstruction section (Section II.E).

Figure 3 shows the equivalent circuit model of the coupling section (L1, L2, and M) and the L-R filter (L3 and R1), which is used as an integrator here. The knee

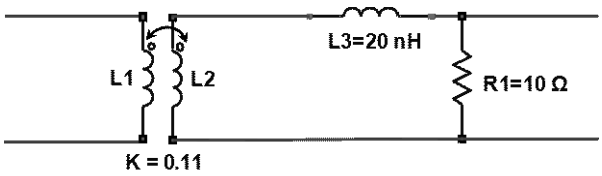


Figure 3: Equivalent circuit diagram of the probe, including the L-R low pass filter.

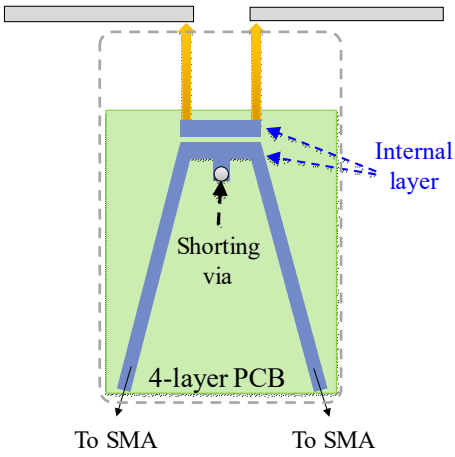


Figure 4: Schematic of the proposed differential probe with shorting via and fixed coupling coefficient, mounted on a trace. (Not drawn to scale.)

frequency (filter pole) of the integrator can be found from equation (2).

$$f_{knee} = \frac{R}{2\pi L} \approx 80\ MHz. \qquad (2)$$

Selection of the knee frequency is a trade-off between ease of filter realization, and error in the reconstructed waveform – Selecting a lower knee frequency means larger bandwidth, more dynamic range, and hence more realization difficulties, while selecting higher knee frequency is translated to weaker integration and introducing more error in the reconstructed waveform. A knee frequency of 80 MHz, for instance, means the filter requires to maintain its -20 dB/decade slope over $log\left(\frac{2\ GHz}{80\ MHz}\right) \approx 1.4$ decades, which is easy to achieve.

Moreover, lowering the pole (knee) frequency reduces the magnitude of the probe response after the knee frequency, which lowers the coupling coefficient. A carelessly selected knee frequency either results in a resonance below 2 GHz or a very weak coupling. Figure 5 compares the frequency response (S21) of the probe circuit model (figure 3) with and without the L-R filter.

## C. PCB Layout

One major drawback of the design shown in figure 2 is its susceptibility to picking up both electric and magnetic fields [5]. To avoid electric field coupling to the probe, differential traces are used and the shorting via is shifted to the middle of the coupled section, as shown in figure 4. This approach effectively shorts out the coupled electric field while letting the

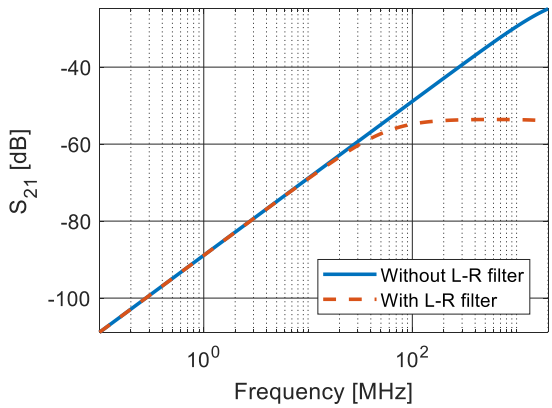


Figure 5: Frequency response of the equivalent circuit model with and without the L-R filter.

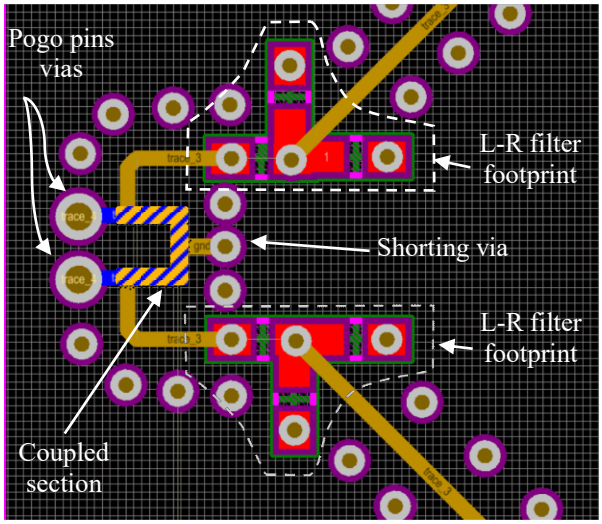


Figure 6: PCB layout of differential probe tip. The coupled section is shown by yellow-blue strips. The coupled traces are 8 mil apart. The indicated bigger vias at the far left are dedicated to the pogo pins; they are not stitching vias. The L-R filter consists of one inductor and two parallel resistors.

coupled magnetic field to reach the output ports. Further suppression of unwanted couplings to the probe is achieved by routing the traces on the mid-layers, using stitching vias and polygons.

Figure 6 shows the layout of the probe tip. (Polygons and other layers are not shown for a better view.) The yellow trace is located on layer 3, and the blue trace is on layer 4 (bottom layer). The transient current enters and exits the coupled section (indicated by strips) through the "pogo pin" vias and the blue trace. The magnetic field is inductively coupled to the yellow trace, which is located on the upper layer. The coupled energy is then integrated by the L-R filter. Figure 7 shows the PCB stack-up of the probe.

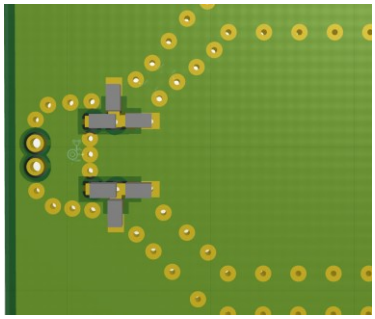

(a)

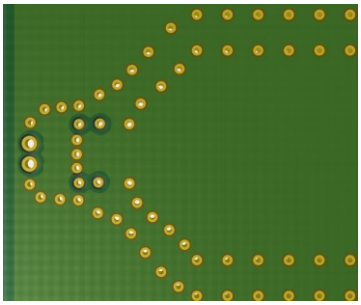

(b)

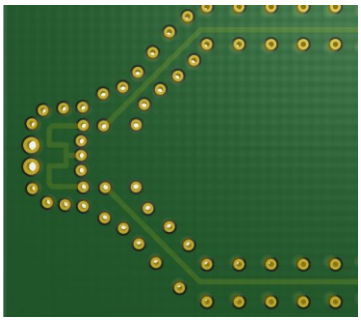

(c)

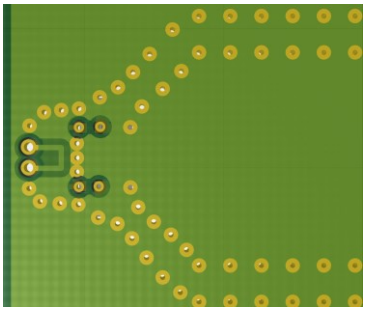

(d)

Figure 7: 3D view of the PCB stack-up; (a) top layer, (b) middle layer 1, (c) middle layer 2, (d) bottom layer.

## D. Equivalent Circuit Model

As shown in figure 3, the coupled section is modeled by L1, L2, and mutual inductance, M. Mutual inductance is proportional to the length of the coupled traces and can be calculated by equation (3).

$$M = K\sqrt{L_1 L_2}, \tag{3}$$

where K is the mutual inductor coupling coefficient and indicates the magnetic flux linkage between L1 and L2. Through full-wave simulation L1, L2, and M can be obtained. While M is a function of L1 and L2, K only depends on the geometry of the coupling section. By selecting K=0.11, one can simply use the length of the coupling section as the value of L1 and L2, in nH; i.e., L1=L2=2.6 nH. Therefore, for modeling other probes with a different coupling length and the same geometry at the coupling section, only the coupling length needs to be adjusted in the model. A probe with a different geometry at the coupling section calls for recalculation of M through full-wave simulation.

## E. Current Reconstruction

The transient current is reconstructed in two steps. First, the L-R filter integrates from the current coupled into the probe (though the coupling section), which is already discussed in Section II-B; then, the probe response is numerically deconvolved from the integrated data in the frequency domain – either measured probe response or simulated probe response can be used. Lack of wideband, noise-free data for FFT and IFFT transformations strongly (and negatively) affects the reconstructed waveform; therefore, simulated probe response is preferred. We use the probe equivalent circuit model and its transfer function for the deconvolution process.

The transfer function, H, can be calculated using equations (4) and (5) assuming a source and a load impedance of 50 Ω. Any mismatch between this model frequency response and the probe response directly affects the reconstructed current. Equation (6) shows how the deconvolution is carried out and the current is reconstructed in the time domain.

$$H(f) = \frac{V_{out}}{V_{in}} = \left[\frac{(50 + j\omega L_1)}{j\omega M}\left(1 + \frac{j\omega L_3}{R_2} + \frac{j\omega L_2}{R_2}\right) - \frac{j\omega M}{R_2}\right]^{-1}, \tag{4}$$

$$R_2 = R_1\frac{50}{R_1 + 50}, \tag{5}$$

where, L1 = L2 = 2.6 nH, L3 = 20 nH, and R1 = 10 Ω (see figure 3).

$$Recontructed\ transient\ current(t) = IFFT\left\{\frac{FFT\{current\ afer\ the\ LR\ filter\}}{H(f)}\right\}. \tag{6}$$

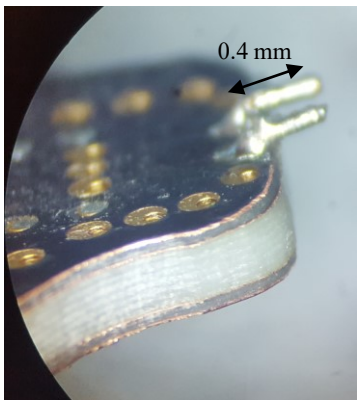


Figure 8: Microscopic view of the fabricated probe. The L-R filter is located on the other side of the board.

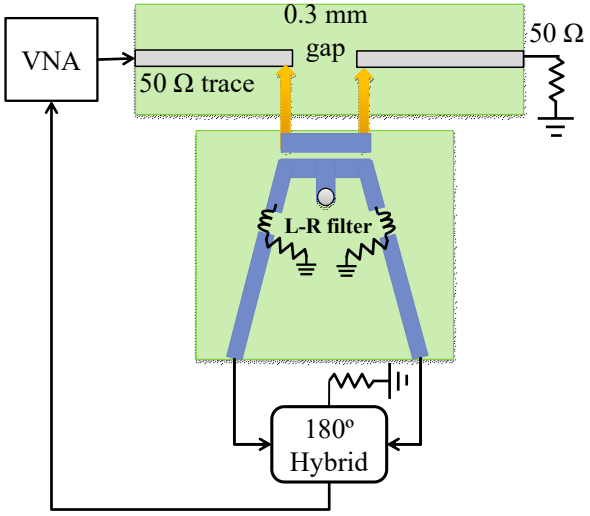


Figure 9: VNA measurement setup to obtain insertion loss of the probe. The transmission lines connecting the probe to the hybrid should be as similar as possible. (Drawing is not to scale.)

In order to remove possible artifacts near DC and remove high-frequency noise, a single-pole high-pass filter with a cut-off frequency of ~300 kHz and a single-pole low-pass filter with a cut-off frequency of ~6 GHz is applied to the data before performing the FFT in equation (6). The imaginary part of this equation is practically zero.

# F. Validation

## 1. Insertion Loss Validation

Figure 8 illustrates the close-up view of the fabricated probe. Figure 9 shows the setup used to obtain the frequency response of the fabricated probe. The 50-Ω trace is 3 mm wide and has a 0.3 mm gap. A wideband, 180º hybrid is used to combine the probe outputs. A hybrid is a matched microwave device with four ports [6]. The signals fed to ports A and B of a

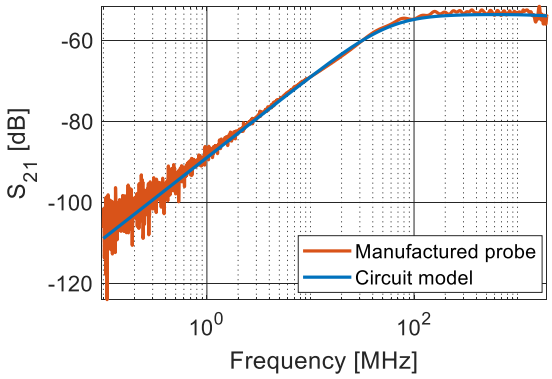


Figure 10: Frequency response of the fabricated probe compared to its circuit model. The probe coupling length is 2.6 mm. The circuit model is shown in figure 3.

180º hybrid are combined in-phase and out-of-phase and appear at the Σ and Δ ports, respectively. To combine the probes differential output, the Δ (out-of-phase) port is used. The Σ port is terminated to 50 Ω.

Figure 10 compares the simulated insertion loss obtained from the model (figure 3) with the measured insertion loss obtained from figure 9. At low frequencies, less energy is coupled to the probe, approaching the VNA noise floor, hence the noisy behavior at low frequencies. The small resonance near 2 GHz is caused by the hybrid; it has a limited bandwidth of 2 GHz.

The effect of the trace width on the measured insertion loss is also studied. It is found that decreasing the trace width from 3 mm to 0.4 mm while maintaining a 50 Ω impedance leads to less than 1 dB difference in insertion loss.

## 2. Transient Current Measurement Validation

Figure 11 shows the measurement setup used to validate the probe readouts. A Tektronix CT1 probe is used to verify the readings of the proposed probe. For this measurement, the 50 Ω impedance is maintained inside the CT1 loop by using a custom-designed coaxial structure. For a differential pair, this approach is not applicable as the differential traces cannot be separated while keeping their differential and common mode impedances intact.

As shown in figure 11, a transmission line pulse generator (TLP) injects a 50 V, 7 ns pulse into the trace. About 1 A of current is expected to be measured by the probes. Figure 12a compares the measured currents by the CT1 and the *Zero-Ohm substitution* probe. The effect of the L-R filter (integrator) can be observed. After deconvolving the probe response from this result, the actual current waveform can be reconstructed,

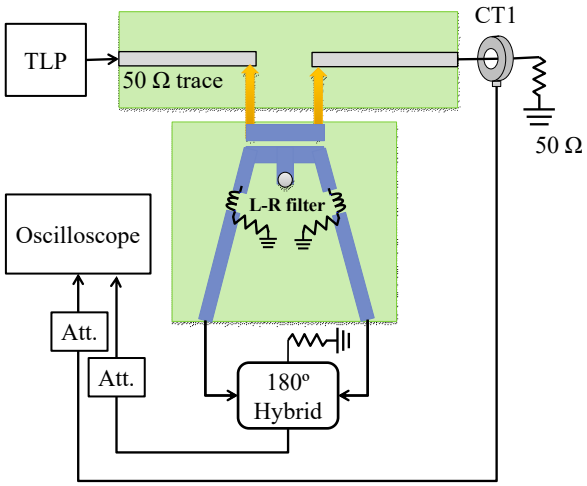


Figure 11: Measurement setup to compare the probe readings with a commercial Tektronix CT1 probe. A custom-built enclosure for the CT1 probe allows for maintaining the 50 Ω impedance while measuring the transient current passed through the CT1 probe.

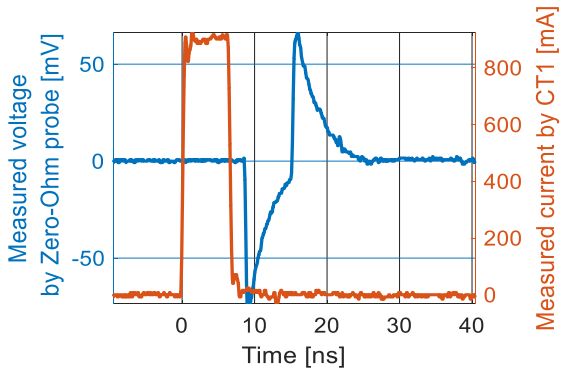


(a)

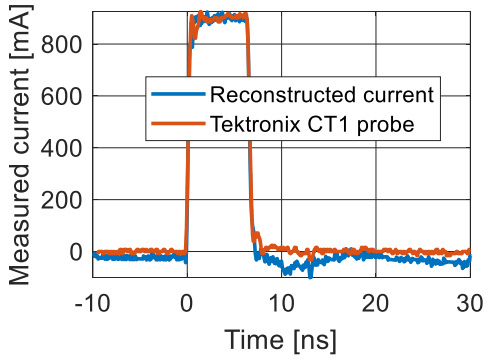


(b)

Figure 12: Comparison between the current measured by CT1 probe and the *Zero-Ohm substitution* probe; (a) CT1 current Vs. unprocessed waveform, (b) CT1 current Vs. reconstructed current. The corresponding measurement setup is shown in figure 11.

shown in figure 12b. A good agreement can be observed.

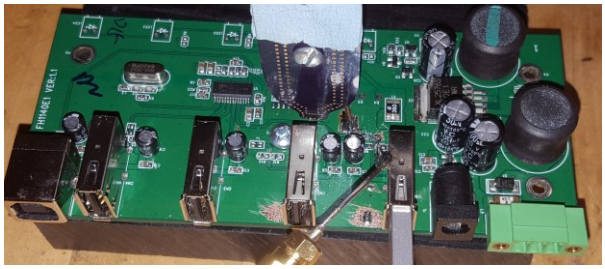

(a)

(b)

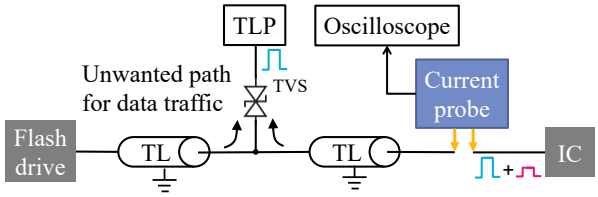


(c)

Figure 13: Setup for measuring the transient current injected into one trace of a differential pair. The DUT is the hub IC. (a) DUT and probe; (b) close-up view of the probe position; (c) block diagram of the injection and the measurement setup. The data is bidirectional. (The hybrid is not shown.)

# III. Application

Figure 13 shows a measurement setup where the probe is used to measure the transient current entering the USB hub IC. A flash drive is connected to the hub and communicates with the IC. A 7-ns pulse is injected into the trace under test using TVS injection method. Refer to [7, 8] for more information about this injection method. As shown in figure 13c, the probe is placed between the injection point and the hub IC to measure the current going into the IC. It is expected that part of the injected current is absorbed by the flash drive on the left and the rest get reflected. The reflected portion will then appear with a delay at the hub IC and is measured by the probe.

Figure 14 shows the transient current going into the hub IC. Data traffic was present on the differential pair

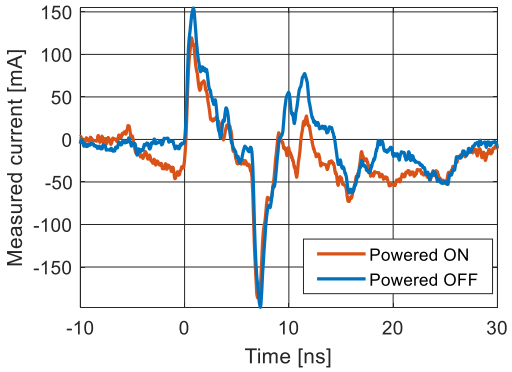


Figure 14: Transient current entering the IC data pin during powered ON and OFF conditions. The negative current before 0 ns is an artifact of the current reconstruction step. This could be addressed by removing any DC bias in the data and increasing number of samples.

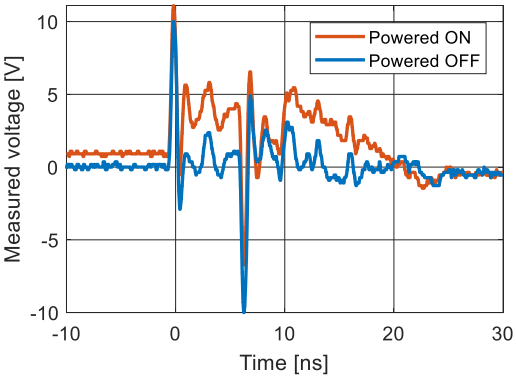


Figure 15: IC pin voltage fluctuation during transient stress under powered ON and OFF conditions.

when the hub was powered ON. The second bump (roughly from 9 to 16 ns) corresponds to the transient current reflected from the flash drive that enters the hub IC after bouncing back. As observed, when powered ON, the flash drive reflects less energy, causing the bump to differ under powered ON and OFF conditions.

Mounting a 1.1 kΩ pick-up resistor (Pick-Tee) at the IC pin, we can observe how the IC pin voltage varies during the transient stress, for powered ON and powered OFF conditions. As shown in figure 15, a DC bias of ~1 V is present on the data trace when the hub IC is powered ON and is visible before the transient event. During the stress, the IC internal protection turns on, limiting the IC pin voltage to ~6 V. After the failure, the DC bias is lost (see the voltage near 30 ns). The stress caused the hub-flash connection to fail. A power cycle was needed to re-establish the connection.

# IV. Summary and Conclusion

Measuring a transient current on a high-speed data trace when in the presence of data traffic is not trivial, as the current monitoring equipment can negatively affect the data transfer rate. This problem can be bypassed by using a magnetic field probe to monitor the transient current; however, the probe's readings might significantly change depending on the probe location, orientation, and distance from the data trace. This paper presents *Zero-Ohm substitution* current probe to drastically reduce these dependencies. As opposed to a magnetic field probe, the presented probe produces stable readings, thanks to its fixed coupling coefficient. The probe was fabricated on a 4-layer FR4 substrate. Its current readings as well as its equivalent circuit model was validated. The proposed probe was used to measure the transient current in the data traces during data transfer.

# V. Acknowledgments

This paper is based upon work supported partially by the National Science Foundation under Grant No. IIP-1916535.

# VI. References

[1] Tektronix. AC Current Probes [Online]. Available: download.tek.com/datasheet/AC_Current_Probes.pdf

[2] Sen Yang, Jianchi Zhou, David Pommerenke, and Dazhao Liu, "A Simple Frequency Response Compensation Method for Current Probe Measurements of Esd Currents," in *2017 IEEE International Symposium on Electromagnetic Compatibility & Signal/Power Integrity (EMCSI)*, 2017, pp. 158-163.

[3] Shubhankar Marathe, Javad Meiguni, Keyu Zhou, David Pommerenke, and Mike Hertz, "Esd Generator Tip Current Reconstruction Using a Current Probe Measurement at the Ground Strap," in *2019 IEEE International Symposium on Electromagnetic Compatibility, Signal & Power Integrity (EMC+ SIPI)*, 2019, pp. 141-146.

[4] Hiroki Funato and Takashi Suga, "Magnetic near-Field Probe for Ghz Band and Spatial Resolution Improvement Technique," in *2006 17th International Zurich Symposium on Electromagnetic Compatibility*, 2006, pp. 284-287.

[5] Sen Yang, Qiaolei Huang, Guanghua Li, Reza Zoughi, and David J Pommerenke, "Differential E-Field Coupling to Shielded H-Field Probe in near-Field Measurements and a Suppression Approach," *IEEE Transactions on Instrumentation and Measurement,* vol. 67, pp. 2872-2880, 2018.

[6] Omid Hoseini Izadi, Ahmad Hosseinbeig, Guanghua Li, and David Pommerenke, "Effects of Mechanical

Tolerances of Usb 2.0 Cables on Skew and Radiated Emission," *IEEE Transactions on Electromagnetic Compatibility,* 2018.
[7] Thomas Schwingshackl, Benjamin Orr, Joost Willemen, Werner Simbürger, Harald Gossner, Wolfgang Bösch, and David Pommerenke, "Powered System-Level Conductive Tlp Probing Method for Esd/Emi Hard Fail and Soft Fail Threshold Evaluation," in *2013 35th Electrical Overstress/Electrostatic Discharge Symposium*, 2013, pp. 1-8.
[8] Charvaka Duvvury and Harald Gossner, *System Level Esd Co-Design*: John Wiley & Sons, 2015.